Tilt Angle Effect on Optimizing HALO PMOS Performance

Jiong-Guang Su, Shyh-Chyi Wong, Chi-Tsung Huang, Chang-Ching Cheng,
Chih-Chiang Wang*, Shiang Huang-Lu*, Bing-Yui Tsui*
Institute of Electrical Engineering and Department of Electronics ,Feng-Chia University,
100 Wen-Hua Rd., Taichung, Taiwan, ROC
*Submicron Technology Group, ERSO, Industrial Technology Research Institute,
Hsin-Chu, Taiwan, ROC

Abstract – Deep submicrometer MOS devices often need special structures to optimize their performance. The HALO structure, or pocket implant, is usually adopted for PMOS to reduce off-state leakage current and enhance on-state drive current. This paper studies the tilt angle effect of HALO implant on device performance. It is found that device with higher tilt angle gives reduced body effect and increased source resistance as compared to those with low tilt angle, and the effect of resistance and body effect compensates each other, resulting equivalent DC performance for different tilt angle. We suggest that based on this equivalence of DC performance, high tilt angle should be adopted for HALO devices due to their lower junction capacitance.

I. INTRODUCTION

Halo structure is a promising architecture for sub-quarter micron technology [1-3]. Several previous works reported that HALO with high tilt angle greatly improves device performance with acceptable off-state leakage(I_{off})[1]. There also exist works claiming that HALO implant will seriously degrade performance (I_{dsat}) due to increased source resistance[3]. The performance limit of HALO devices and determination of tilt angle hence is a critical issue and open problem. In this paper, a new investigation on tilt angle of HALO PMOS is presented. It is found that tilt angle of HALO implant does not affect the final device performance (I_{dsat} and I_{off}) if proper dose is adopted. This performance equivalence of various tilt angle is due to the self compensation between body factor and source resistance. Based on this result, high tilt angle should be adopted because of its small junction capacitance.

II. EXPERIMENT

The process flow used in our experiment is summarized in Table I, and the symbol " * " in the Halo-implant block denotes the parameter to be adjusted. The simulated device cross-section with doping concentration contours is shown in Fig.1, and split conditions are shown in Table II. The effect of various tilt angles, including of 0°, 15°, 30° and 40° , are studied with various HALO implant doses to explore their performance limit. All HALO implants are with energy of 130 KeV. The gate length is

TABLE I
PROCESS FLOW

PROCESS STEP	PROCESS CONDITIONS
P-type formation	<100> , Boron concentration:1.3e15cm^{-3}
N-well formation	material/dose/energy: Ph/1.3e13cm^{-2}/460keV
Channel implant	material/dose/energy: Ph/2e12cm^{-2}/40keV
Gate oxide	thickness:55 Å
Poly deposition	thickness:0.1 μm\length:0.18 μm
Halo implant	material/dose/energy/tilt : As/*cm^{-2}/130keV/*degree
LDD implant	material/dose/energy:BF$_2$/1e13cm^{-2}/25keV
Spacer formation	length:0.08 μm
P$^+$ S/D implant	material/dose/energy: BF$_2$/2e15cm^{-2}/30keV

MEDICI[5] are used in this analysis. To obtain reliable process simulation, all implantation model parameters, damage model and diffusion model parameters have been calibrated with SIMS data[6], with both as-implant profile calibration and after-annealing profile calibration. Lateral scattering parameters were determined by Monte-Carlo analysis. For device simulation, mobility

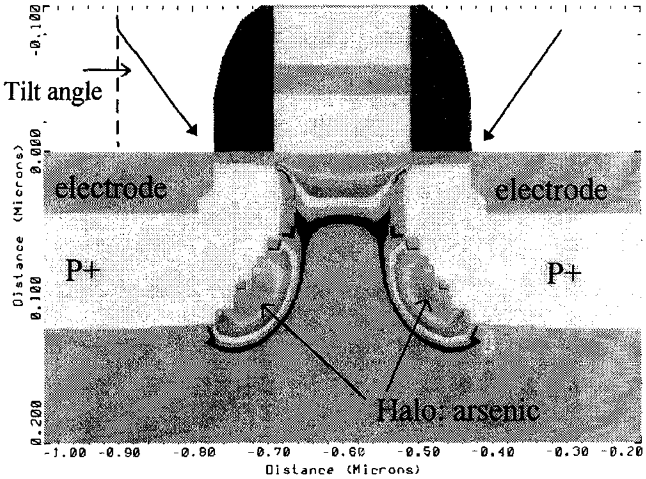

Fig. 1 The Halo PMOS cross-section.

0-7803-3775-1/97/$10.00

TABLE II
SPLIT CONDITION

split number	HALO implant condition	
	dose #/cm^{-2}	tilt degree
A	3e12	0°
B	7e12	0°
C	9e12	0°
D	1e12	15°
E	3e12	15°
F	5e12	15°
G	1e12	30°
H	2e12	30°
I	3e12	30°
J	5.2e12	30°
K	8.5e11	40°
L	1e12	40°
M	2e12	40°
N	3e12	40°

model parameters, including both vertical field degradation and velocity saturation[5], have been calibrated with devices from a 0.25um technology with 0.18μm, gate oxide thickness of 55Å, LDD dose of $10^{13}/cm^2$ with 25KeV, and nitride spacer of 0.08μm. The process simulator TSUPREM4 [4] and device simulator similar thermal cycles. To define the device performance target, we extract the off-state leakage current I_{off} from bias on V_{gs}= -0.1V,V_{ds}= -1.8V,and on-state drive current I_{dsat} from V_{gs}= -1.8V,V_{ds}=-1.9V.

III.RESULTS AND DISCUSSIONS

In Fig.2(a), a scatter plot of I_{dsat} versus I_{off} for various tilt angle and implant doses are presented. It is observed that all splits lie on one unified trend line, indicating that different tilt angle will eventually give identical DC performance, i.e., same I_{dsat} with similar I_{off}, provided that proper HALO implant dose has been adopted. Based on the above observation, we suggest that tilt angle of HALO implant does not affect ultimate device performance. This statement is further verified in Fig. 2(b)-(c). Here, we define a novel figure of merit parameter $S=(\delta I_{dsat}/\delta I_{off})$, indicating the sensitivity of drive current versus off-state leakage current. Note that the parameter S can be further decomposed into two parameters S_1 and S_2 ($S=S_1 x S_2$), with $S_1=(\delta I_{dsat}/\delta Dose)$ and $S_2=(\delta Dose/\delta I_{off})$. It is clearly shown in Fig. 2(b)-(c) that $S_1(40^0)=-4.1x10^{-17}$, $S_1(15^0)=-3x10^{-17}$, $S_2(40^0)=-5.26x10^{11}$and $S_2(15^0)=-7.2x10^{11}$. Hence $|S_1(40°)| > |S_1(15°)|$, and $|S_2(40°)| < |S_2(15°)|$ in Fig.2(b)-(c). As a result, S(15°) is approximately equal to S(40°), pointing out that HALO with tilt angle of 15° and 40° lie in the same I_{dsat}-I_{off} trend line, demonstrating the fact that tilt angle does not affect final performance.

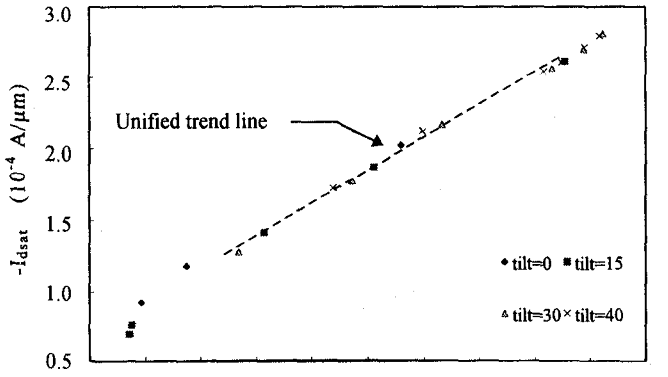

Fig. 2(a) The I_{off} versus I_{dsat} with different tilt and dose.

The equivalence of device performance for various tilt angle is further explored by analyzing two electrical parameters: Gamma (body factor parameter) and Rs(source resistance). The motivation for analyzing Gamma and Rs is based on the fact that the doping

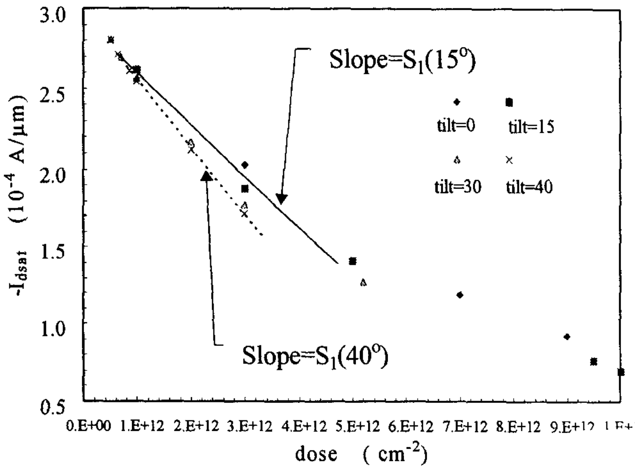

Fig.2 (b) The pocket implant dose versus I_{dsat}.

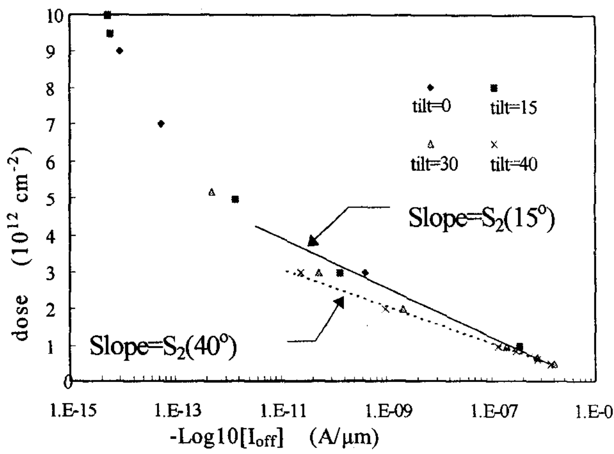

Fig. 2(c) The I_{off} versus implant dose.

distribution in devices with 40° HALO and 15° HALO is obviously different, and the performance equivalence should be due to a self-compensation of several different mechanisms, which will be discussed as follows. The body factor parameter Gamma is calculated by taking the average depletion charge density in the Gamma-calculation-box near drain as shown in Fig. 3,and using the following equations

$$\gamma \equiv \sqrt{2 q \varepsilon_s \overline{N_d}} / C'_{ox} \tag{1}$$

where $\overline{N_d}$ is the average depletion charge and define as

$$\frac{\iint_{xy} N_d \, dx \, dy}{\iint_{xy} dx \, dy} \tag{2}$$

In (1), C'_{ox} is the gate oxide capacitance, q is unit charge density, and ε_s is the Silicon dielectric constant. The source resistance Rs is evaluated based on distribution of quasi-Fermi potential ϕ_{qf} and the formula $Rs=(\delta\phi_f'/I_{dsat})$. Here, $\delta\phi_f'$ is the weighted mean of ϕ_{qf} with current density as the weighting parameter[7], and define as

$$\delta\phi_f' = \frac{\sum \Phi_{qf} J}{\sum J} \tag{3}$$

Note that Rs is divided into three sections and $Rs=R_1+R_2+R_3$, denoting diffusion resistance, drain crowding resistance, and drain-channel junction crowding resistance respectively. Obviously R_3 dominates Rs and is used in our analysis here. Also note here that leakage current path is on the surface, and HALO pocket on the surface is required reduce this I_{off}. Comparing splits E(15°) and N(40°) in Fig. 4, we find that similar I_{dsat} is shown with same dose (both $3 \times 10^{12}/cm^2$). Note that here the calculated Gamma for 40° is much lower than 15° due to fact that the HALO pocket for 40° is localized near device surface, resulting a smaller Gamma. The phenomenon that HALO implant is placed near surface squeezes the channel, thinning the conduction layer near source and drain junction, resulting higher source resistance as shown in Table III, where R_3 of split N is higher than R3 of split E. The correlation of I_{dsat} and R_3 is shown in Fig. 5, demonstrating the strong influence of R_3 on degrading I_{dsat}. Considering the effects of both Gamma and Rs, we suggest that devices with 40°-HALO shows smaller gamma and higher Rs as compared to the devices with 15°-HALO, and finally giving similar performance (I_{dsat}, I_{off}) as the 15°-HALO. Fig.6 shows the threshold voltage versus dose with differential tilt angles.

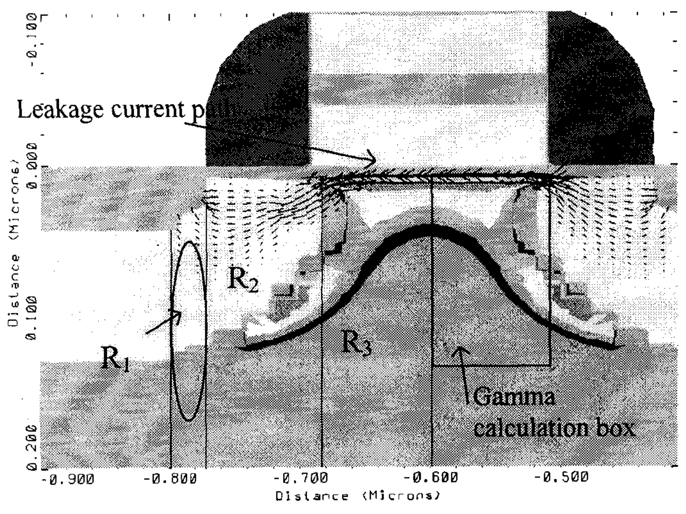

Fig.3 The leakage current path, three regions for calculate resistance and the gamma calculation box.

TABLE III

THE CORRELATION OF RESISTANCE AND GAMMA

split	R1(Ω)	R2(Ω)	R3(Ω)	Total Res.(Ω)	gamma($V^{1/2}$)
A	5.28	268	1526	1799	0.3794
B	3.41	161	2486	2650	0.5320
C	2.25	115	3379	3497	0.5947
D	4.95	366	1111	1482	0.3022
E	2.44	300	1599	1902	0.4419
F	4.21	195	2101	2300	0.5466
G	4.91	365	1137	1507	0.2753
H	4.54	269	1437	1711	0.3342
I	4.93	290	1665	1959	0.3858
J	3.91	180	2288	2472	0.4789
K	4.91	355	1123	1483	0.2529
L	4.85	356	1157	1518	0.2613
M	4.44	259	1479	1743	0.3109
N	3.99	271	1725	2000	0.3548

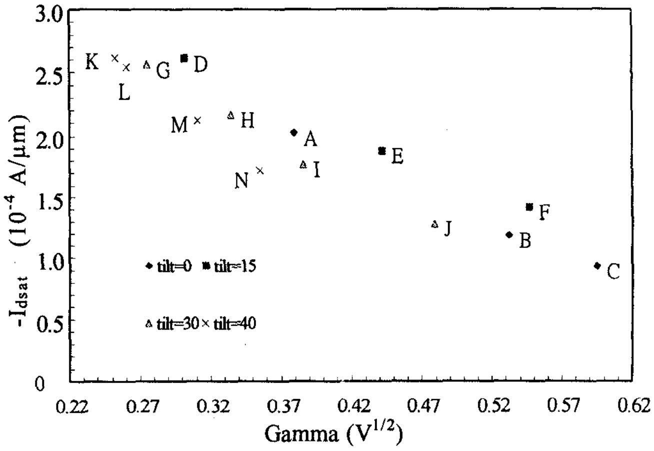

Fig. 4 The gamma versus I_{dsat}.

Again higher sensitivity of threshold voltage versus implant dose is shown for devices with higher implant tilt angle, demonstrating that HALO doses near surface (from the high tilt angle) strongly influences threshold voltage.

IV.COCLUSION

In summary, we investigate the influence of tilt angle of HALO implant on optimizing PMOS performance based on process and device simulation. The result indicates that different tilt angle of HALO implant results similar performance if proper dose is adopted, and this conclusion is different from existing works[1,2,3]. This results is further verified by the extracted body factor parameter Gamma and resistance R3, with the effects of these two parameters compensating each other. Based our study, large tilt angle of HALO implant should be adopted to get reduced parasitic capacitance and enhanced device performance.

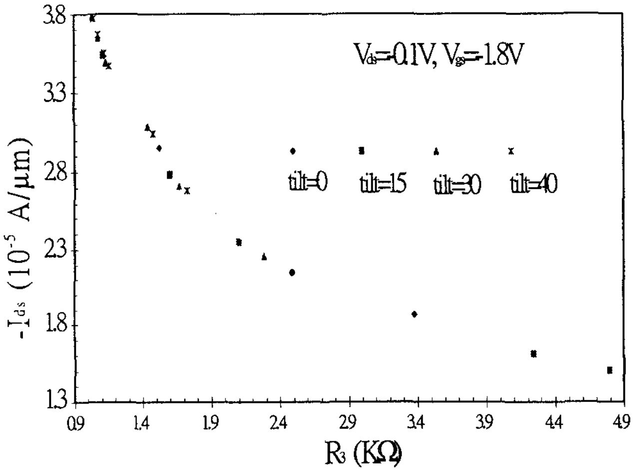

Fig. 5 The resistance with different tilts.

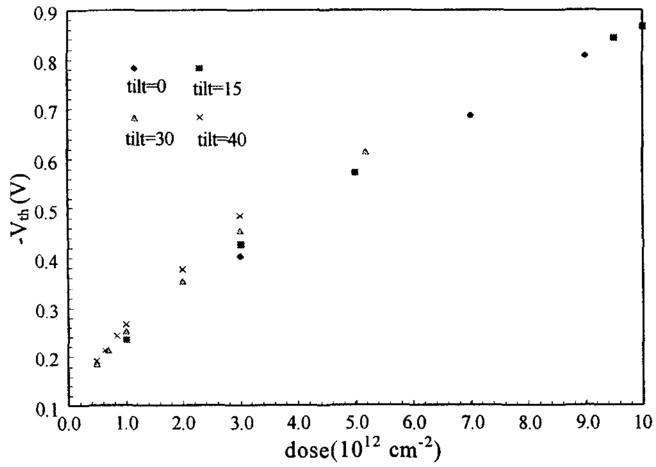

Fig. 6 Threshold voltage versus dose.

REFERENCES

[1] M. Rodder, Q. Z. Hong,M. Nandakumar, S. Aur, J.C. Hu, I.-C. Chen, *IEDM Tech. Dig.* 1996, pp. 563-566.

[2] Prashant Shamarao, et al. IEEE ED-43,1996.

[3] Hyunsang Hwang, Dong-Hoon Lee and Jeong Mo Hwang, *IEDM Tech. Dig.* 1996, pp.567-570.

[4] Technology Modeling Associates, Inc., "TSUPREM-4 User's Manual," August 1994.

[5] Technology Modeling Associates, Inc., "MEDICI User's Manual," August 1994.

[6] M. Simard-Normandin and C. Slaby, "Empirical Modeling of Low Energy Boron Implants in Silicon," *J. Electrochem. Soc.* ,pp. 2218-2223, September, 1985.

[7] G. S. Samudra, B. P. Seah and C.H. Ling, "Determination of LDD MOSFET Drain Resistance From Device Simulation," *Solid-State Electronics*, Vol.39,No.5,pp.753-758,1996.